

Numerical Generation of Images for the Gibbs Phenomenon Near a Corner in the Plane

Alia Khurram, *Member, IAENG*, and David W Kammler

Abstract—In this paper we have studied the Gibbs ripples associated with an α -corner, i.e., the indicator function for the smaller region of \mathbb{R}^2 bounded by two rays from the origin that intersect at the angle α , $0 < \alpha < \pi$. (Such corners cannot occur in the univariate case.) We have done this by removing from the Fourier representation all components that lie outside of a disk with radius $\sigma \geq 0$. We have used a technique to rearrange the approximating integrals in a form that facilitates efficient computation. We then produced two dimensional images for the Gibbs ripples that correspond to the corner angles $\alpha = \pi/3, \pi/2, 2\pi/3, \pi$. We observed that the maximum overshoot occurs near the corner.

Index Terms—Gibbs Phenomena, Fourier Transform, Bivariate Analysis.

I. INTRODUCTION

AT the close of the nineteenth century the physicists A.A. Michelson and S.W. Stratton constructed a mechanical harmonic analyzer that could plot graphs for trigonometric polynomials with up to 80 terms [11]. After producing many plots of partial sums for Fourier series of periodic functions with jump discontinuities, they observed that all such approximations exhibit annoying “ripples” near every point of discontinuity. J.W. Gibbs provided an informal analysis of this phenomenon [4] which now bears his name [5], [6]. An earlier exposition was given by Wilbraham [7] in 1841.

Gibbs ripples are produced by removing the high frequency components from the Fourier representation of a function that has a jump discontinuity. If the function is periodic, this involves truncating the corresponding Fourier series. If the function is aperiodic, this involves a similar truncation of the Fourier integral representation. This phenomenon has been studied in several dimensions [2], [9]. An evident manifestation of the phenomenon is a rippling effect which is undesirable in some applications. For example, in reconstruction of magnetic resonance imaging (MRI) data, methods are being developed to remove the Gibbs ringing artifact that occurs at the boundaries of tissues [1], [8].

Moving from univariate to bivariate functions, there are several important new features to consider. If the function has a jump discontinuity across a smooth curve in its domain, one might reasonably expect to produce Gibbs ripples analogous to those from the univariate case. A less predictable phenomenon occurs when the function has a jump discontinuity across a corner where two smooth curves in the domain intersect at some angle α , $0 < \alpha < \pi$. A recent paper of G. Helmbert [6] analyzes the Gibbs phenomenon at such a

corner in the case where the function is doubly periodic. Helmbert’s approximation deletes all components that lie outside of a square in frequency space. In contrast, we remove high frequency components by deleting from the Fourier representation all terms having an index that exceeds some threshold.

II. THE GIBBS PHENOMENON FOR THE HEAVISIDE STEP IN \mathbb{R}^1

A suitably regular function $f(x)$ on \mathbb{R} has the Fourier representation

$$f(x) = \int_{s=-\infty}^{\infty} F(s)e^{2\pi isx} ds, \quad (1)$$

where the Fourier transform F is given by

$$F(s) := \int_{x=-\infty}^{\infty} f(x)e^{-2\pi isx} dx. \quad (2)$$

If we suppress all frequencies $|s| < \sigma$, we obtain the low pass approximation

$$f_{\sigma}(x) := \int_{s=-\sigma}^{\sigma} F(s)e^{2\pi isx} ds, \quad \sigma > 0. \quad (3)$$

We can use the unit box

$$\text{rect}(s) := \begin{cases} 1 & \text{if } -1/2 < s < 1/2 \\ 0 & \text{otherwise,} \end{cases} \quad (4)$$

to remove the high frequency components from (1). Indeed, since

$$\text{rect}\left(\frac{s}{2\sigma}\right) = \begin{cases} 1 & \text{if } |s| < \sigma \\ 0 & \text{otherwise,} \end{cases} \quad (5)$$

we see that

$$f_{\sigma}(x) = \int_{s=-\infty}^{\infty} F(s) \text{rect}\left(\frac{s}{2\sigma}\right) e^{2\pi isx} ds. \quad (6)$$

The functions $F(s)$ and $\text{rect}(s/2\sigma)$ are the Fourier transforms of $f(x)$ and $2\sigma \text{sinc}(2\sigma x)$, respectively, so we can use the convolution rule for Fourier transforms to see that

$$f_{\sigma}(x) = f(x) * 2\sigma \text{sinc}(2\sigma x),$$

or equivalently

$$f_{\sigma}(x) = \int_{u=-\infty}^{\infty} f(u) \frac{\sin[2\pi\sigma(x-u)]}{\pi(x-u)} du. \quad (7)$$

We are interested in studying the behavior of such a low pass approximation near a point of jump discontinuity, so we will replace f by the Heaviside step function

$$h(x) = \begin{cases} 1 & \text{if } x > 0 \\ 1/2 & \text{if } x = 0 \\ 0 & \text{if } x < 0. \end{cases} \quad (8)$$

Manuscript received July 24, 2013; revised November 30, 2013.

A. Khurram is in the Mathematics Department at Adrian College, Adrian, MI, 49221 USA e-mail: (akhurram@adrian.edu).

David Kammler is professor emeritus at Southern Illinois University Carbondale, Carbondale, IL 62901.

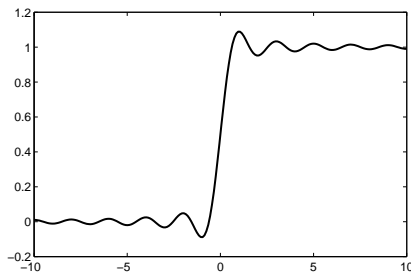


Fig. 1. The low pass approximation $g(x) = h_\sigma(\frac{x}{2\sigma})$ for the Heaviside step (8)

The low pass approximation (7) for this function is

$$h_\sigma(x) = \int_{u=0}^{\infty} \frac{\sin[2\pi\sigma(x-u)]}{\pi(x-u)} du. \tag{9}$$

We shall find it convenient to work with the dilate

$$\begin{aligned} h_\sigma\left(\frac{x}{2\sigma}\right) &= \int_{u=0}^{\infty} \frac{\sin[\pi(x-2\sigma u)]}{\pi(x-2\sigma u)} 2\sigma du \\ &= \int_{u=0}^{\infty} \frac{\sin[\pi(x-u)]}{\pi(x-u)} du, \end{aligned}$$

which is independent of σ . With this in mind, we define the univariate Gibbs function

$$g(x) := h_\sigma\left(\frac{x}{2\sigma}\right) = \int_{u=0}^{\infty} \frac{\sin[\pi(x-u)]}{\pi(x-u)} du. \tag{10}$$

The oscillating integrand in (10) decreases like $1/u$ as $u \rightarrow \infty$. Thus the improper integral converges, but it converges much too slowly to evaluate by direct numerical integration. We take $x > 0$ and use the known definite integral [10] p. 62

$$\int_{u=-\infty}^0 \frac{\sin(\pi u)}{\pi u} du = \int_{u=0}^{\infty} \frac{\sin(\pi u)}{\pi u} du = \frac{1}{2}, \tag{11}$$

to rewrite (10) in the form

$$\begin{aligned} g(x) &= \int_{u=0}^x \frac{\sin[\pi(x-u)]}{\pi(x-u)} du + \int_{u=x}^{\infty} \frac{\sin[\pi(x-u)]}{\pi(x-u)} du \\ &= \int_{u=0}^x \frac{\sin(\pi u)}{\pi u} du + \int_{u=0}^{\infty} \frac{\sin(\pi u)}{\pi u} du \\ &= \frac{1}{2} + \int_{u=0}^x \text{sinc}(u) du. \end{aligned} \tag{12}$$

We can use numerical quadrature to evaluate the remaining integral in (12).

The Gibbs function g is shown in Fig. (1). The characteristic Gibbs ripples are evident. The function g has maxima of 1.089, 1.033, 1.020, ... at $x = 1, 3, 5, \dots$ respectively and minima of 0.951, 0.974, 0.983, ... at $x = 2, 4, 6, \dots$, respectively. The maximum Gibbs overshoot is a bit less than 9% of the unit jump in h .

III. THE GIBBS PHENOMENON FOR AN α -CORNER IN \mathbb{R}^2

We will now extend the analysis from the previous section to a two dimensional context. A suitably regular bivariate function f on \mathbb{R}^2 has the Fourier representation

$$f(x, y) = \int_{u=-\infty}^{\infty} \int_{v=-\infty}^{\infty} F(u, v) e^{2\pi i(ux+vy)} dv du \tag{13}$$

where the bivariate Fourier transform is given by

$$F(u, v) := \int_{x=-\infty}^{\infty} \int_{y=-\infty}^{\infty} f(x, y) e^{-2\pi i(ux+vy)} dy dx. \tag{14}$$

We will suppress all frequencies u, v outside the disk $u^2 + v^2 \leq \sigma^2$ to obtain the low pass approximation

$$f_\sigma(x, y) := \iint_{u^2+v^2 \leq \sigma^2} F(u, v) e^{2\pi i(ux+vy)} dv du. \tag{15}$$

We will use the unit diameter cylinder

$$\text{cyl}(u, v) := \begin{cases} 1 & \text{if } u^2 + v^2 < 1/4 \\ 0 & \text{otherwise,} \end{cases} \tag{16}$$

to write

$$f_\sigma(x, y) = \iint_{uv} F(u, v) \text{cyl}\left(\frac{u}{2\sigma}, \frac{v}{2\sigma}\right) e^{2\pi i(ux+vy)} dv du. \tag{17}$$

The radially symmetric function $\text{cyl}(x, y)$ is the Fourier transform of the radially symmetric function $\text{jinc}(\sqrt{x^2 + y^2})$, where

$$\text{jinc}(r) := \begin{cases} 1 & \text{if } r = 0 \\ J_1(\pi r)/2r & \text{if } r > 0, \end{cases}$$

and where, J_1 is the first order Bessel function [3], p.359.

$$J_1(r) := \int_0^1 e^{-2\pi i x} e^{i r \sin 2\pi x} dx,$$

Since the functions $F(u, v)$ and $\text{cyl}(\frac{u}{2\sigma}, \frac{v}{2\sigma})$ are the Fourier transforms of $f(x, y)$ and $(2\sigma)^2 \text{jinc}(2\sigma\sqrt{x^2 + y^2})$, respectively, we can use the two dimensional convolution rule to see that

$$f_\sigma(x, y) = f(x, y) * (2\sigma)^2 \text{jinc}(2\sigma\sqrt{x^2 + y^2}),$$

or equivalently

$$f_\sigma(x, y) = \iint_{pq} \sigma f(p, q) \frac{J_1[2\pi\sigma\sqrt{(x-p)^2 + (y-q)^2}]}{\sqrt{(x-p)^2 + (y-q)^2}} dq dp. \tag{18}$$

We are interested in studying the behavior of such a low pass approximation near ‘‘edges’’ and ‘‘corners’’ where f has a jump discontinuity. With this in mind, we select a corner angle α with $0 < \alpha < 2\pi$ and define the α -corner function

$$C_\alpha(x, y) := \begin{cases} 1 & \text{if } -\alpha/2 < \arg(x, y) < \alpha/2 \\ 1/2 & \text{if } \arg(x, y) = \pm\alpha/2 \\ & \text{and } (x, y) \neq (0, 0) \\ \alpha/2\pi & \text{if } (x, y) = (0, 0) \\ 0 & \text{otherwise.} \end{cases} \tag{19}$$

Here $\arg(x, y)$ is the smaller angle between the ray joining $(0, 0)$ to (x, y) and the positive x-axis as shown in Fig. 2. Thus $C_\alpha(x, y)$ is the indicator function of a wedge from \mathbb{R}^2 that has the corner angle α (with suitable average values on the edge and vertex, cp.(8).)

It can be seen from (19) and Fig. 2 that two such corner functions with vertex angles α and $2\pi - \alpha$ can be combined as

$$C_\alpha(x, y) + C_{2\pi-\alpha}(-x, y) = 1. \tag{20}$$

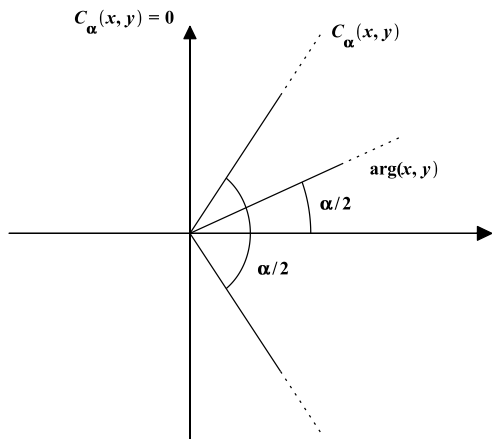


Fig. 2. The α -corner in R^2 that corresponds to (19)

The low pass approximation (18) satisfies the corresponding identity

$$C_{\alpha,\sigma}(x, y) + C_{2\pi-\alpha,\sigma}(-x, y) = 1,$$

or equivalently

$$C_{\alpha,\sigma}(x, y) = 1 - C_{2\pi-\alpha,\sigma}(-x, y).$$

This identity allows us to express the $C_{\alpha,\sigma}$ for a “large” α with $\pi < \alpha < 2\pi$ in terms of the $C_{\alpha,\sigma}$ for a “small” α with $0 < \alpha < \pi$. From now on we will assume that $0 < \alpha \leq \pi$.

We will use

$$S_\alpha := \{(x, y) : C_\alpha(x, y) \neq 0\}$$

for the support of C_α , and use (18), (19) to write

$$C_{\alpha,\sigma}(x, y) = \iint_{S_\alpha} \sigma \frac{J_1[2\pi\sigma\sqrt{(x-p)^2 + (y-q)^2}]}{\sqrt{(x-p)^2 + (y-q)^2}} dqdp. \tag{21}$$

Since the cone S_α is unchanged by a 2σ -dilation, we find

$$C_{\alpha,\sigma}\left(\frac{x}{2\sigma}, \frac{y}{2\sigma}\right) = \iint_{S_\alpha} \frac{J_1[\pi\sqrt{(x-p)^2 + (y-q)^2}]}{2\sqrt{(x-p)^2 + (y-q)^2}} dqdp. \tag{22}$$

The integral of (22) does not depend on σ , so we can define the bivariate Gibbs function

$$g_\alpha(x, y) := C_{\alpha,\sigma}\left(\frac{x}{2\sigma}, \frac{y}{2\sigma}\right) = \iint_{S_\alpha} \frac{J_1[\pi\sqrt{(x-p)^2 + (y-q)^2}]}{2\sqrt{(x-p)^2 + (y-q)^2}} dqdp \tag{23}$$

(that serves as a two dimensional generalization of (10).)

The Bessel function J_1 has the asymptotic formula

$$J_1(r) \approx \sqrt{\frac{2}{\pi}} \frac{\cos(r - 3\pi/4)}{\sqrt{r}} \quad \text{when } r \gg 1, \tag{24}$$

[3] p.359, so it is easy to see that the integral converges conditionally but not absolutely. We will now show how to rewrite (23) in a form suitable for numerical integration.

IV. NUMERICAL ANALYSIS OF THE GIBBS PHENOMENON AT AN EDGE IN \mathbb{R}^2

We first consider the case where $\alpha = \pi$. Using (23) we write

$$g_\pi(x, y) = \int_{p=0}^\infty \int_{q=-\infty}^\infty \frac{J_1[\pi\sqrt{(x-p)^2 + (y-q)^2}]}{2\sqrt{(x-p)^2 + (y-q)^2}} dqdp. \tag{25}$$

This integral is independent of y so we will work with

$$g_\pi(x, 0) = \int_{p=0}^\infty \int_{q=-\infty}^\infty \frac{J_1[\pi\sqrt{(x-p)^2 + q^2}]}{2\sqrt{(x-p)^2 + q^2}} dqdp. \tag{26}$$

We will rewrite (26) in a form that facilitates numerical integration. As a first step, we write

$$\begin{aligned} g_\pi(x, 0) &= \int_{p=0}^x \int_{q=-\infty}^\infty \frac{J_1[\pi\sqrt{(x-p)^2 + q^2}]}{2\sqrt{(x-p)^2 + q^2}} dqdp \\ &\quad + \int_{p=x}^\infty \int_{q=-\infty}^\infty \frac{J_1[\pi\sqrt{(x-p)^2 + q^2}]}{2\sqrt{(x-p)^2 + q^2}} dqdp \\ &= \int_{p=0}^x \int_{q=-\infty}^\infty \frac{J_1[\pi\sqrt{p^2 + q^2}]}{2\sqrt{p^2 + q^2}} dqdp \\ &\quad + \int_{p=0}^\infty \int_{q=-\infty}^\infty \frac{J_1[\pi\sqrt{p^2 + q^2}]}{2\sqrt{p^2 + q^2}} dqdp. \end{aligned} \tag{27}$$

Using symmetry and the Fourier synthesis equation (13) for the function (16) we see that

$$\begin{aligned} &\int_{p=0}^\infty \int_{q=-\infty}^\infty \frac{J_1[\pi\sqrt{p^2 + q^2}]}{2\sqrt{p^2 + q^2}} dqdp \\ &= \frac{1}{2} \int_{p=-\infty}^\infty \int_{q=-\infty}^\infty \frac{J_1[\pi\sqrt{p^2 + q^2}]}{2\sqrt{p^2 + q^2}} dqdp \\ &= \frac{1}{2} \text{cyl}(0, 0) = \frac{1}{2}, \end{aligned} \tag{28}$$

so we can write (27) in the form

$$g_\pi(x, 0) = \frac{1}{2} + \int_{p=0}^x \int_{q=-\infty}^\infty \frac{J_1[\pi\sqrt{p^2 + q^2}]}{2\sqrt{p^2 + q^2}} dqdp. \tag{29}$$

The integral is an odd function of x , so we will only consider the case where $x \geq 0$.

We will introduce polar coordinates to exploit the radial symmetry of the integrand. We remove a quarter circle from the half-strip $0 < p < x, q > 0$ as shown in Fig. 3, and thereby see that

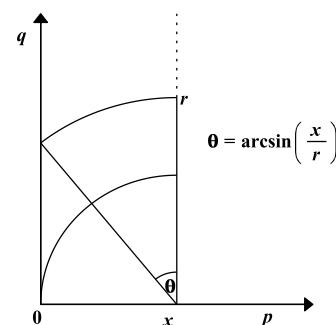


Fig. 3. The region of integration for (29)

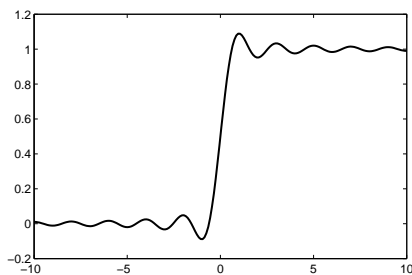


Fig. 4. The function $g_\pi(x, 0)$ from (31)

$$\begin{aligned} & \int_{p=0}^x \int_{q=-\infty}^{\infty} \frac{J_1[\pi\sqrt{p^2+q^2}]}{2\sqrt{p^2+q^2}} dqdp \\ &= 2 \int_{r=0}^x \int_{\theta=0}^{\pi/2} \frac{J_1(\pi r)}{2r} r drd\theta \\ &+ 2 \int_{r=x}^{\infty} \int_{\theta=0}^{\arcsin(\frac{x}{r})} \frac{J_1(\pi r)}{2r} r drd\theta \\ &= \frac{\pi}{2} \int_{r=0}^x J_1(\pi r) dr + \int_{r=x}^{\infty} \arcsin\left(\frac{x}{r}\right) J_1(\pi r) dr. \end{aligned} \tag{30}$$

In this way we express

$$g_\pi(x, 0) = \frac{1}{2} + \frac{\pi}{2} \int_{r=0}^x J_1(\pi r) dr + \int_{r=x}^{\infty} \arcsin\left(\frac{x}{r}\right) J_1(\pi r) dr \tag{31}$$

in terms of two univariate integrals.

Using (24) we see that the integrand from the last term of (31) has the asymptotic form

$$\begin{aligned} & \arcsin\left(\frac{x}{r}\right) J_1(\pi r) \\ & \approx \arcsin\left(\frac{x}{r}\right) \sqrt{\frac{2}{\pi}} \frac{\cos(r - 3\pi/4)}{\sqrt{r}} \text{ when } r \gg 1 \\ & \approx \sqrt{\frac{2}{\pi}} x r^{-3/2} \cos(r - 3\pi/4) \text{ when } r \gg x. \end{aligned} \tag{32}$$

Thus the improper integral from (31) converges absolutely but very slowly. Since the integrand oscillates, we can use the alternating series bound from calculus to see that the truncation error has the approximate bound

$$\left| \int_L^\infty \arcsin\left(\frac{x}{r}\right) J_1(\pi r) dr \right| \leq \left| \int_L^{L+1} \arcsin\left(\frac{x}{r}\right) J_1(\pi r) dr \right|, \tag{33}$$

so we might expect a truncation error of $O(L^{-3/2})$. With a bit of care we can get a much smaller bound. We choose L so that $\pi(L - 3/4) = N\pi$ (where the cosine takes the value ± 1). The truncation error (33) will then be of $O(L^{-5/2})$.

We used MATLAB to evaluate the integral from (31) and plot the function $g_\pi(x, 0)$. The resulting graph is shown in Fig. (4). As expected, we find

$$g_\pi(x, 0) = g(x), \tag{34}$$

i.e., the error for a jump discontinuity at an “edge” in the bivariate case is the same as that for a jump discontinuity at a step in the univariate case. Such agreement helps to confirm the correctness of our analysis and the accuracy of the numerical integrations from (31). (Our MATLAB codes for evaluating (12) and (31) produce numerical results that agree to six decimal places.)

V. NUMERICAL ANALYSIS OF THE GIBBS PHENOMENON AT AN α -CORNER IN \mathbb{R}^2

We will now simplify the integral (23) when $0 < \alpha \leq \pi$. From the reflection symmetry of S_α we obtain the corresponding symmetry

$$g_\alpha(x, y) = g_\alpha(x, -y), \tag{35}$$

for the Gibbs function. From now on we will replace y by $|y|$ before we evaluate g_α so that we can assume $y \geq 0$.

Using the radial symmetry of the integrand and the synthesis equation (13) for the cylinder we see that

$$\begin{aligned} & \iint_{S_\alpha} \frac{J_1[\pi\sqrt{p^2+q^2}]}{2\sqrt{p^2+q^2}} dqdp = \int_{r=0}^\infty \int_{\theta=-\alpha/2}^{\alpha/2} \frac{J_1(\pi r)}{2r} r drd\theta \\ &= \frac{\alpha}{2\pi} \int_{r=0}^\infty \int_{\theta=-\pi}^\pi \frac{J_1(\pi r)}{2r} r drd\theta \\ &= \frac{\alpha}{2\pi} \text{cyl}(0, 0) = \frac{\alpha}{2\pi}. \end{aligned} \tag{36}$$

Of course, when $\alpha = \pi$, this gives the integral $\frac{1}{2}$ from (28).

Now let

$$S_\alpha(x, y) = \{(p, q) \in \mathbb{R}^2 : (p - x, q - y) \in S_\alpha\} \tag{37}$$

be the (x, y) translate of the cone S_α in \mathbb{R}^2 as shown in Fig.5.

(The tip of the cone S_α is translated to the point (x, y) .)

Using (36) we write (23) in the form

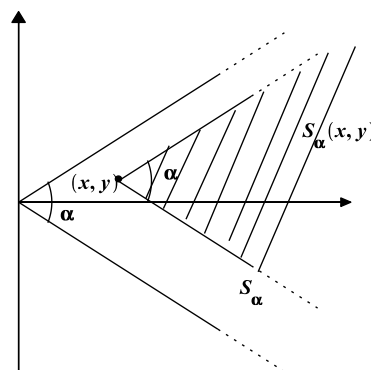


Fig. 5. The translate $S_\alpha(x, y)$ of the cone S_α

$$\begin{aligned} g_\alpha(x, y) &= \iint_{S_\alpha} \frac{J_1[\pi\sqrt{(x-p)^2+(y-q)^2}]}{2\sqrt{(x-p)^2+(y-q)^2}} dqdp \\ &= \frac{\alpha}{2\pi} + \iint_{S_\alpha} \frac{J_1[\pi\sqrt{(x-p)^2+(y-q)^2}]}{2\sqrt{(x-p)^2+(y-q)^2}} dqdp \\ &\quad - \iint_{S_\alpha(x,y)} \frac{J_1[\pi\sqrt{(x-p)^2+(y-q)^2}]}{2\sqrt{(x-p)^2+(y-q)^2}} dqdp. \end{aligned} \tag{38}$$

Let (R, Θ) denote the polar representation of (x, y) , i.e.

$$R := \sqrt{x^2 + y^2} \text{ and } \Theta := \begin{cases} \arctan(y/x) & \text{if } x > 0, \\ \pi/2 & \text{if } x = 0, \\ \pi - \arctan(y/|x|) & \text{if } x < 0. \end{cases} \tag{39}$$

We will now find an alternative representation for the difference of the integrals from (38). In so doing, we will deal separately with situations where $0 < \alpha \leq \pi/2$ and where $\pi/2 \leq \alpha \leq \pi$.

Consider first the situation where $0 < \alpha \leq \pi/2$. We must evaluate the difference of integrals over regions S_α and $S_\alpha(x, y)$. We will express the difference in terms of integrals over certain semiinfinite strips, with each strip being bounded by the line segment joining $(0, 0)$ to (x, y) , by a bounding ray for the cone S_α and by a parallel bounding ray for the cone $S_\alpha(x, y)$. Fig. V shows such strips R_1, R_2, \dots, R_{10} . The sign we associate with the upper strip integral changes when $\Theta = \alpha/2$ and the sign we associate with the lower strip integral changes when $\Theta = \pi - \alpha/2$. The lower strip has a square edge when $\Theta = \pi/2 - \alpha/2$ and the upper strip has a square edge when $\Theta = \pi/2 + \alpha/2$. Using the regions of Fig. V we write

$$g_\alpha(x, y) = \frac{\alpha}{2\pi} + \begin{cases} \iint_{R_1} dm + \iint_{R_2} dm & \text{if } 0 \leq \Theta \leq \alpha/2 \\ -\iint_{R_3} dm + \iint_{R_4} dm & \text{if } \alpha/2 < \Theta \leq \pi/2 - \alpha/2 \\ -\iint_{R_5} dm + \iint_{R_6} dm & \text{if } \pi/2 - \alpha/2 < \Theta \leq \pi/2 + \alpha/2 \\ -\iint_{R_7} dm + \iint_{R_8} dm & \text{if } \pi/2 + \alpha/2 < \Theta \leq \pi - \alpha/2 \\ -\iint_{R_9} dm - \iint_{R_{10}} dm & \text{if } \pi - \alpha/2 < \Theta \leq \pi, \end{cases} \quad (40)$$

where in each case

$$dm = \frac{J_1[\pi\sqrt{(x-p)^2 + (y-q)^2}]}{2\sqrt{(x-p)^2 + (y-q)^2}} dqdp. \quad (41)$$

We will now simplify (40). We find it helpful to use

$$\begin{aligned} d_+ &:= |x \sin(\alpha/2) - y \cos(\alpha/2)|, \\ d_- &:= |x \sin(\alpha/2) + y \cos(\alpha/2)|, \end{aligned} \quad (42)$$

for the distances from the point (x, y) to the lines

$$\begin{aligned} y \cos(\alpha/2) &= x \sin(\alpha/2), \\ y \cos(\alpha/2) &= -x \sin(\alpha/2), \end{aligned} \quad (43)$$

respectively. Each of the regions R_1, R_2, \dots, R_{10} can be written as the sum or difference of a half strip \mathcal{H}_d and a triangle $\mathcal{T}_{d,R}$ as shown in Fig. 7. (We use a sum when the angle at $(0, 0)$ is acute and a difference when the angle is obtuse). The integrand is invariant under a rotation or reflection about the point (x, y) , so we can orient these regions to simplify the integration.

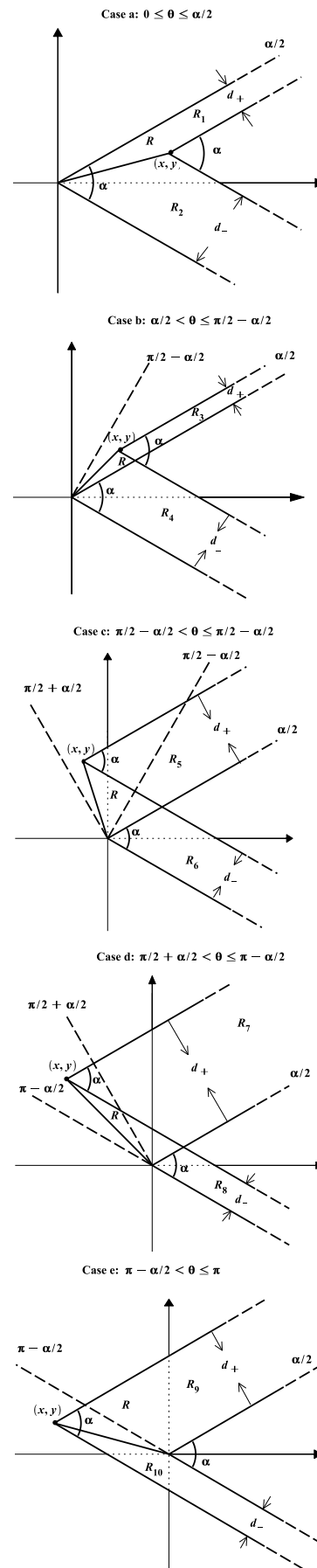


Fig. 6. Regions associated with S_α and $S_\alpha(x, y)$ when $0 < \alpha \leq \pi/2$

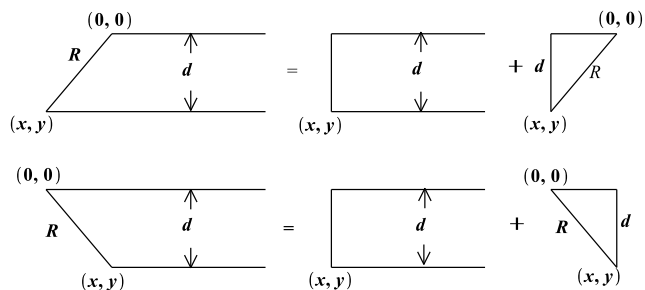


Fig. 7. Decomposition of the regions R_1, R_2, \dots, R_{10} using the half strip $\mathcal{H}_d(x, y)$ and the triangle $\mathcal{T}_{d,R}(x, y)$

When we integrate (41) over the half strip

$$\mathcal{H}_d(x, y) := \{(x, y) + (p, q) : 0 < p < \infty, 0 < q < d\},$$

we can use symmetry with (29) and (34) to see that

$$\begin{aligned} H(d) &:= \iint_{\mathcal{H}_d(x,y)} \frac{J_1[\pi\sqrt{(x-p)^2 + (y-q)^2}]}{2\sqrt{(x-p)^2 + (y-q)^2}} dqdp \\ &= \frac{1}{2} \int_{q=0}^d \int_{p=-\infty}^{\infty} \frac{J_1[\pi\sqrt{p^2 + q^2}]}{2\sqrt{p^2 + q^2}} dqdp \\ &= \frac{1}{2} \left\{ g_\pi(d, 0) - \frac{1}{2} \right\} = \frac{1}{2} \left\{ g(d) - \frac{1}{2} \right\} \\ &= \frac{1}{2} \int_{u=0}^d \text{sinc}(u) du. \end{aligned} \tag{44}$$

We can evaluate $H(d)$ by numerically integrating the well behaved sinc function.

When we integrate (41) over the triangle

$$\mathcal{T}_{d,R}(x, y) := \left\{ (x, y) + (p, q) : 0 < q < d, \right. \\ \left. 0 < p < q\sqrt{R^2 - d^2/d} \right\}$$

we use polar coordinates with the regions shown in Fig. 8 to write

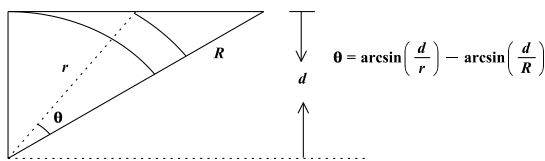


Fig. 8. Splitting $\mathcal{T}_{d,R}$ into regions for polar integration

$$\begin{aligned} T(d, R) &:= \iint_{\mathcal{T}_{d,R}(x,y)} \frac{J_1[\pi\sqrt{(x-p)^2 + (y-q)^2}]}{2\sqrt{(x-p)^2 + (y-q)^2}} dqdp \\ &= \left\{ \frac{\pi}{2} - \arcsin\left(\frac{d}{R}\right) \right\} \int_0^d \frac{J_1(\pi r)}{2} dr \\ &\quad + \int_d^R \left\{ \arcsin\left(\frac{d}{r}\right) - \arcsin\left(\frac{d}{R}\right) \right\} \frac{J_1(\pi r)}{2} dr. \end{aligned} \tag{45}$$

We can evaluate $T(d, R)$ by numerically evaluating the two univariate integrals.

We now use the functions (44) and (45) with (40) and the regions R_1, R_2, \dots, R_{10} from Fig. V to see that

$$g_\alpha(x, y) = \frac{\alpha}{2\pi} + \begin{cases} H(d_+) + T(d_+, R) + H(d_-) + T(d_-, R) & \text{when } 0 \leq \Theta \leq \alpha/2 \\ -H(d_+) - T(d_+, R) + H(d_-) + T(d_-, R) & \text{when } \alpha/2 < \Theta \leq \pi/2 - \alpha/2 \\ -H(d_+) - T(d_+, R) + H(d_-) - T(d_-, R) & \text{when } \pi/2 - \alpha/2 < \Theta \leq \pi/2 + \alpha/2 \\ -H(d_+) + T(d_+, R) + H(d_-) - T(d_-, R) & \text{when } \pi/2 + \alpha/2 < \Theta \leq \pi - \alpha/2 \\ -H(d_+) + T(d_+, R) - H(d_-) + T(d_-, R) & \text{when } \pi - \alpha/2 < \Theta \leq \pi. \end{cases} \tag{46}$$

We can further simplify equation (46) by using the function

$$\text{sgn}(x) := \begin{cases} 1 & \text{if } x > 0 \\ 0 & \text{if } x = 0 \\ -1 & \text{if } x < 0. \end{cases} \tag{47}$$

Indeed, we change the sign associated with the integral over the upper, lower strip as Θ passes through $\alpha/2, \pi - \alpha/2$, respectively, and we change the sign associated with the triangle from the upper, lower strip as Θ passes through $\pi/2 + \alpha/2, \pi/2 - \alpha/2$, respectively. This being the case, we can write

$$\begin{aligned} g_\alpha(x, y) &= \frac{\alpha}{2\pi} \\ &\quad + \text{sgn}\left[\sin\left(\frac{\alpha}{2} - \Theta\right)\right] \left\{ H(d_+) + \text{sgn}\left[\cos\left(\frac{\alpha}{2} - \Theta\right)\right] T(d_+, R) \right\} \\ &\quad + \text{sgn}\left[\sin\left(\frac{\alpha}{2} + \Theta\right)\right] \left\{ H(d_+) + \text{sgn}\left[\cos\left(\frac{\alpha}{2} + \Theta\right)\right] T(d_+, R) \right\} \\ &\quad \quad \quad 0 \leq \alpha \leq \pi/2. \end{aligned} \tag{48}$$

We now consider the situation where $\pi/2 \leq \alpha \leq \pi$. Again the sign associated with the integral over the upper, lower strip changes as Θ passes through $\alpha/2, \pi - \alpha/2$, respectively, and the sign associated with the triangle from the upper, lower strip changes as Θ passes through $\pi/2 + \alpha/2, \pi/2 - \alpha/2$, respectively. Fig. 9 shows the various regions R_1, R_2, \dots, R_{10} when $\pi/2 \leq \alpha \leq \pi$.

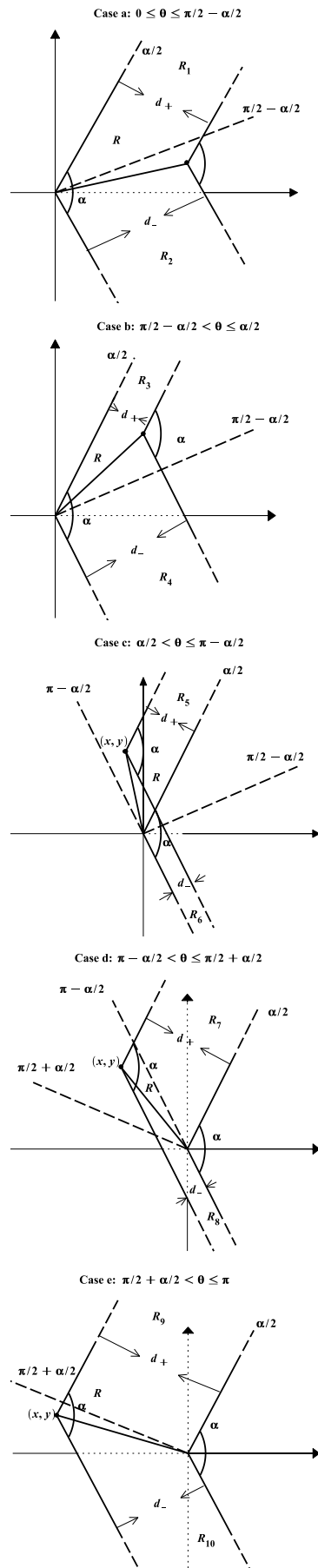


Fig. 9. Regions associated with S_α and $S_\alpha(x, y)$ when $0 < \alpha \leq \pi/2$

Using these regions we write

$$g_\alpha(x, y) = \frac{\alpha}{2\pi} + \begin{cases} \iint_{R_1} dm + \iint_{R_2} dm & \text{if } 0 \leq \Theta \leq \pi/2 - \alpha/2 \\ \iint_{R_3} dm + \iint_{R_4} dm & \text{if } \pi/2 - \alpha/2 < \Theta \leq \alpha/2 \\ -\iint_{R_5} dm + \iint_{R_6} dm & \text{if } \alpha/2 < \Theta \leq \pi - \alpha/2 \\ -\iint_{R_7} dm + \iint_{R_8} dm & \text{if } \pi - \alpha/2 < \Theta \leq \pi/2 + \alpha/2 \\ -\iint_{R_9} dm - \iint_{R_{10}} dm & \text{if } \pi/2 + \alpha/2 < \Theta \leq \pi, \end{cases} \quad (49)$$

where in each case dm is given by (41). We now use (44) and (45) with (49) to write

$$g_\alpha(x, y) = \frac{\alpha}{2\pi} + \begin{cases} H(d_+) + T(d_+, R) + H(d_-) + T(d_-, R) & \text{when } 0 \leq \Theta \leq \pi/2 - \alpha/2 \\ H(d_+) + T(d_+, R) + H(d_-) - T(d_-, R) & \text{when } \pi/2 - \alpha/2 < \Theta \leq \alpha/2 \\ -H(d_+) - T(d_+, R) + H(d_-) - T(d_-, R) & \text{when } \alpha/2 < \Theta \leq \pi - \alpha/2 \\ -H(d_+) - T(d_+, R) - H(d_-) + T(d_-, R) & \text{when } \pi - \alpha/2 < \Theta \leq \pi/2 + \alpha/2 \\ -H(d_+) + T(d_+, R) - H(d_-) + T(d_-, R) & \text{when } \pi/2 + \alpha/2 < \Theta \leq \pi. \end{cases} \quad (50)$$

or equivalently

$$g_\alpha(x, y) = \frac{\alpha}{2\pi} + \operatorname{sgn} \left[\sin \left(\frac{\alpha}{2} - \Theta \right) \right] \left\{ H(d_+) + \operatorname{sgn} \left[\cos \left(\frac{\alpha}{2} - \Theta \right) \right] T(d_+, R) \right\} + \operatorname{sgn} \left[\sin \left(\frac{\alpha}{2} + \Theta \right) \right] \left\{ H(d_+) + \operatorname{sgn} \left[\cos \left(\frac{\alpha}{2} + \Theta \right) \right] T(d_+, R) \right\} \quad \pi/2 \leq \alpha \leq \pi. \quad (51)$$

We observe that (51) is the same as (48).

We have written MATLAB codes to evaluate and plot g_α for various values of the corner angle α . We evaluate g_α at each point x, y with

$$\begin{aligned} x &= -4.00, -3.98, \dots, 5.98, 6.00 \\ y &= 0.01, 0.03, \dots, 4.97, 4.99. \end{aligned} \quad (52)$$

For each (x, y) from (52) we use (39) and (42) to evaluate Θ, R, d_+, d_- . We then use MATLAB to compute the strip integrals $H(d_+), H(d_-)$ and the triangle integrals $T(d_+, R), T(d_-, R)$ by numerically evaluating the corresponding integrals (44), (45) using a tolerance 10^{-6} (which is sufficient to show the structure of the Gibbs phenomenon.) We then use (48) or (51) to obtain $g_\alpha(x, y)$ at each of the points (52). Finally, we use the symmetry (34) to obtain values of $g_\alpha(x, -y)$ corresponding to the points (52). In this way we obtain a matrix G of ordinates $g_\alpha(x, y)$ for points (x, y) near a corner. We then use MATLAB to display G . Fig.10 shows the surface $g_\alpha(x, y)$ that corresponds to the right angle corner with $\alpha = \pi/2$.

After some experimentation, we have found that a good way to visualize the Gibbs ripples is to display an intensity plot for the error

$$e_\alpha(x, y) := g_\alpha(x, y) - C_\alpha(x, y). \quad (53)$$

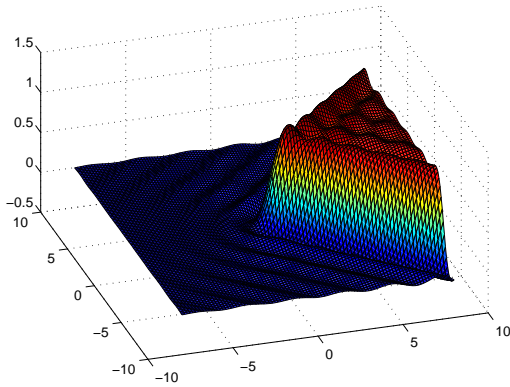


Fig. 10. Surface plot of the Gibbs function g_α when $\alpha = \pi/2$

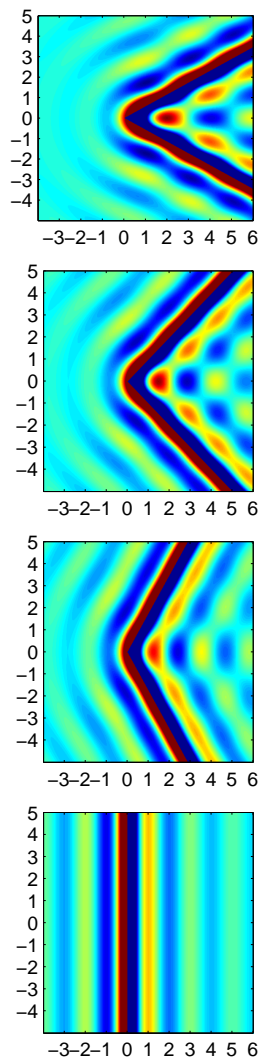


Fig. 11. Regions associated with S_α and $S_\alpha(x, y)$ when $0 < \alpha \leq \pi/2$

Fig.11, shows intensity plots for Gibbs ripples where $\alpha = \pi/3, \pi/2, 2\pi/3, \pi$ respectively. We see the intensity interference pattern that is formed when the (univariate) Gibbs ripples associated with the edges of $C_\alpha(x, y)$ are combined.

REFERENCES

- [1] R. Archibald and A. Gelb, "A Method to Reduce the Gibbs Ringing Artifact in MRI Scans While Keeping Tissue Boundary Integrity", *IEE Transactions of Medical Imaging*, Vol. 21, No. 4, 2002
- [2] G. Benke, "The Gibbs Phenomenon in Higher Dimensions", *Harmonic Analysis and Applications, Applied and Numerical Analysis 2006*, pp. 3-16.
- [3] R. N. Bracewell, "Two-Dimensional Imaging", *Prentice-Hall, Englewood Cliffs, NJ, 1995*.
- [4] J. W. Gibbs, "Nature", *Volume 58, 1898*, pp. 544-545, *Volume 59, 1898*, pp. 600, and *Volume 59, 1898*, pp. 606.
- [5] G. Helmborg, "A Corner Point Gibbs Phenomenon for Fourier Series in Two Dimensions", *Journal of Approximation Theory 1999*, pp. 1-43.
- [6] G. Helmborg, "Localization of a Corner-Point Gibbs Phenomenon for Fourier Series in Two Dimensions", *Journal of Fourier Analysis and Applications 2002*, pp. 29-41.
- [7] E. Hewitt and R. E. Hewitt, "The Gibbs-Wilbraham Phenomenon: An Episode in Fourier Analysis", *Arch. History Exact Sci. 1979*, pp. 129-160.
- [8] X. Huang and W. Chen, "A Fast Algorithm to Reduce Gibbs Ringing Artifact in MRI", *Proceedings of the 2005 IEEE, Engineering in Medicine and Biology 27th Annual Conference, Shanghai, China, 2005*
- [9] A. J. Jerri, "Advances in the Gibbs Phenomenon", *Sampling Publishing, Potsdam, NY, 2011*.
- [10] D. W. Kammler, "A First Course in Fourier Analysis", *Cambridge University Press, Cambridge, 2007*.
- [11] A. A. Michelson and S. W. Stratton, "A New Harmonic Analyzer", *The American Journal of Science, Fourth Series 1898*, pp. 1-13.